Environmental Science & Technology

pubs.acs.org/est

Article

Biological Responses of Pacific Herring Embryos to Crude Oil Are Quantifiable at Exposure Levels Below Conventional Limits of Quantitation for PAHs in Water and Tissues

John P. Incardona,* Tiffany L. Linbo, James R. Cameron, Barbara L. French, Jennie L. Bolton, Jacob L. Gregg, Carey E. Donald, Paul K. Hershberger, and Nathaniel L. Scholz

Cite This: *Environ. Sci. Technol.* 2023, 57, 19214−19222

Read Online

ACCESS | Metrics & More | Article Recommendations | Supporting Information

ABSTRACT: Pacific herring (*Clupea pallasii*), a cornerstone of marine food webs, generally spawn on marine macroalgae in shallow nearshore areas that are disproportionately at risk from oil spills. Herring embryos are also highly susceptible to toxicity from chemicals leaching from oil stranded in intertidal and subtidal zones. The water-soluble components of crude oil trigger an adverse outcome pathway that involves disruption of the physiological functions of cardiomyocytes in the embryonic herring heart. In previous studies, impaired ionoregulation (calcium and potassium cycling) in response to specific polycyclic aromatic hydrocarbons (PAHs) corresponds to lethal embryolarval heart failure or subtle chamber malformations at the high and low ends of the PAH exposure range, respectively. Sublethal cardiotoxicity, which involves an abnormal outgrowth (ballooning) of the cardiac ventricular chamber soon after hatching, subsequently compromises juvenile heart structure and function, leading to pathological hypertrophy of the ventricle and reduced individual fitness, measured as cardiorespiratory performance. Previous studies have not established a threshold for these sublethal and delayed-in-time effects, even with total (∑)PAH exposures as low as 29 ng/g of wet weight (tissue dose). Here, we extend these earlier findings showing that (1) *cyp1a* gene expression provides an oil exposure metric that is more sensitive than typical quantitation of PAHs via GC−MS and (2) heart morphometrics in herring embryos provide a similarly sensitive measure of toxic response. Early life stage injury to herring (impaired heart development) thus occurs below the quantitation limits for PAHs in both water and embryonic tissues as a conventional basis for assessing oil-induced losses to coastal marine ecosystems.

KEYWORDS: *petroleum pollution, AOP, NRDA, forage fish, fish embryology, heart development, biomarkers, morphometrics*

1. INTRODUCTION

Pacific herring have long been a focal species for studying crude oil toxicity to marine fish, dating back to the ecosystem-scale natural injury assessments that followed the 1989 *Exxon Valdez* oil spill in Prince William Sound, Alaska.[1−5] In the decades since, studies using oiled gravel effluent methods to generate controlled chemical leaching established broadly quantitative exposure−response relationships for biological end points at the molecular, cellular, organ, and whole animal scales. Delayed-in-time toxicity has also been a major focus area, whereby sublethal embryonic abnormalities propagate through hatching and early larval development, with subsequent reductions in individual fitness in surviving juveniles.[6−8] These herring studies, combined with similar findings from a wide range of fish species globally,[9−13] identified the heart and cardiovascular system as the primary target of acute and latent petroleum developmental toxicity. Importantly, end points that measure cardiac function or cardiac morphology, which are closely intertwined, show statistically robust and highly repeatable dose−response relationships for measures of polycyclic aromatic hydrocarbons (PAHs) in both exposure waters and embryonic tissues.[14−16]

Received: May 30, 2023
Revised: October 19, 2023
Accepted: October 20, 2023
Published: November 14, 2023

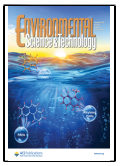

Despite these major leaps forward in understanding how fish early life stages respond to spilled oil, the exposure dimension of natural resource injury assessments has changed very little over the past 30 years. In the early 1990s, environmental levels of PAHs in Prince William Sound water, sediments, and organismal tissues were typically quantified by gas chromatography/mass spectrometry (GC/MS).[2,17−19] Similar methods were used to characterize exposure following more recent spills, with examples including the 2002 *Prestige* spill in Spain,[20] the 2007 *Hebei Spirit* spill in South Korea,[11] the 2010 Deepwater Horizon disaster in the Gulf of Mexico,[10,12] and the 2015 Refugio Beach spill in Southern California.[21] In the present study, we explore whether these conventional analytical methods for PAHs and other petroleum-derived compounds are sufficiently sensitive to determine thresholds for injury in fish, particularly "damage" predicated on novel forms of developmental cardiotoxicity including fitness losses that are delayed-in-time.

Fertilized herring embryos normally develop to hatch over a period of about 2 weeks (12−15 days at ∼9−10 °C). The heart tube forms initially in a lateral orientation and produces irregular contractions by 4.5 days postfertilization (dpf). A regular heartbeat is established the following day, and cardiac organogenesis occurs thereafter (6−10 dpf), whereby the heart rotates into an anterior-posterior orientation, the atrioventricular canal becomes clearly demarcated, and the atrium folds in dorsally at the atrioventricular junction (chamber looping). The ventricle remains a mostly linear tube until hatch, whereafter the chamber begins a rapid posterior outgrowth or ballooning. During the early larval developmental phase, as ballooning progresses, the simple single-layer myocardium of the ventricle begins to form inward projections, or trabeculae, that ultimately make up the inner spongy myocardium of the mature heart. By juvenile stages, the heart is mostly spongy myocardium, surrounded by a multilayered compact myocardium. As in zebrafish,[22] the overall shape of the heart is established in late larvae. Thereafter, the proliferative addition of new cells simply increases the heart size as the animal grows to adulthood.

Because heart function and form are inseparable during development, perturbation of cardiomyocyte function in oil-exposed embryos leads to altered morphogenetic trajectories, which in turn lead to delayed-in-time impairments at later life stages. Based on average molecular weights of component PAHs, crude oil-derived mixtures with total aqueous (∑)PAH concentrations in the nanomolar range disrupt both K^+ and Ca^{2+} ion fluxes that regulate cardiomyocyte action potentials and excitation-contraction coupling.[23] Consequently, abnormal contractility leads to altered fluid dynamics within the forming cardiac chambers, in turn directly and indirectly affecting key cell shape changes and migrations that further refine the ongoing shaping of the heart.[8,9,24,25] As has been detailed extensively in zebrafish,[26−28] the molecular and cellular pathways that integrate normal contractile function with morphogenesis have multiple direct and indirect links with intracellular Ca^{2+} handling. Consequently, the phenotypic effects of oil exposure on herring heart development closely mirror the phenotypic effects of genetic disruption of these pathways in zebrafish.[8,24] In both species, defects in ventricular ballooning and trabeculation lead to nonlethal impairments of embryolarval heart form and pathological hypertrophy at later life stages.[7,8,29] At the same time, with complete loss of function for some genes in zebrafish (e.g., encoding contractile proteins[30]) or exposure to the higher end of oil concentrations,[6,25,31,32] severe cardiac defects lead to embryolarval mortality.

For crude oil exposure, this variation in specific end points depends on the effective PAH dosing for water and tissues. Prior studies in herring covered a tissue ∑PAH dose range of 29−8100 ng/g wet weight,[6−8] which corresponds to roughly 0.14−39 μM for the sake of comparison to the aforementioned in vitro physiological studies. Those rapid, direct effects of crude oil mixtures on critical cardiomyocyte ion fluxes occurred at a very low ∑PAH IC_{50} dose range of 0.17−0.29 μM.[23] This falls at the extreme low end of the embryonic tissue dose range for robust cardiotoxicity in terms of dysregulating both the form and function of the developing heart. Across an upper dose range of ∑PAH 620−8100 ng/g, acute exposures during early to middle stages of cardiac organogenesis (8 dpf) led to a dose-dependent reduction in heart rate (bradycardia), an increase in heartbeat irregularity, and a reduction in chamber contractility.[6] Tissue ∑PAH concentrations of ≥3000 ng/g (∼14 μM) were lethal to embryos by the hatching stage. Conversely, exposures to ∑PAH at concentrations ≤240 ng/g (∼1.2 μM) did not significantly reduce hatch rates, allowing assessment of downstream impacts on heart development.[7,8] Across this lower dose range of 29−240 ng/g wet weight, oil exposures produced a robust and dose-dependent reduction in the degree of ventricular ballooning measured at hatch.[8] The chamber did eventually expand posteriorly by the 2nd week posthatch, but defects in the trabeculation process were subsequently evident in larvae at 67 dpf, followed by hypertrophy of the spongy myocardium in early juveniles at 125 dpf. Consistent with these delayed anatomical defects, herring embryos that survived a ∑PAH body burden of 29 ng/g (∼0.14 μM) and were subsequently grown out in clean seawater for 9 months showed subtle alterations in juvenile ventricular shape and consequent reductions in swimming performance.[7] Consequently, transient and trace exposures to mixtures containing PAHs trigger a pathological hypertrophic remodeling of the developing heart, initiated later in life secondary to delayed ventricular ballooning and defective trabeculation in planktonic larvae.

We recently observed the same effect on ventricular ballooning in a distantly related species with a very different final heart structure, Atlantic haddock.[13] This species showed a similar sensitivity, with an effect at the lowest tested ∑PAH concentrations of 0.1 and 27 ng/g in water and tissues, respectively. Importantly, this was observed with a geologically distinct crude oil (Norwegian Sea Heidrun), using an entirely different exposure route: whole oil droplets dispersed into the water column.[13] In both herring and haddock, the induction of mRNA for the PAH-metabolizing enzyme cytochrome P4501A (CYP1A) was quantified at these low-level exposures. However, CYP1A plays no role in crude oil cardiotoxicity as demonstrated by gene knockdown studies in zebrafish, and instead plays a protective role in detoxification.[33,34] Nevertheless, measures of *cyp1a* mRNA are clearly readily quantifiable exposure metrics for bioavailable PAHs in tissues.

Across 3 decades of oil spill research on marine forage fish, the whole-organ developmental impacts observed at the hatching stage (and later) are readily related to the preceding degree of cardiac dysfunction caused by oil-derived PAHs. However, previous studies have not fully characterized the lower end of the exposure−response range for sublethal cardiotoxicity, with the goal of establishing a no-effect concentration. Here, we use oiled gravel preparations from a prior study, further weathering experimental PAH generator columns to produce even lower

https://doi.org/10.1021/acs.est.3c04122
Environ. Sci. Technol. 2023, 57, 19214−19222

exposure levels for embryonic herring, that is, spanning the limits of quantitation (LOQ) for PAHs in water and tissues. We used the PAH-inducible expression of *cyp1a* as a tissue-dose exposure metric and cardiac chamber anatomy at hatch as a biological effect measure. Compared with the most widely used, conventional chemical analyses for PAHs in both water and tissues, the biological measures were more sensitive.

2. MATERIALS AND METHODS

2.1. Production of Herring Embryos. Ripe herring were captured by the Washington Department of Fish and Wildlife on April 20, 2017, by gill net from the Cherry Point stock in northern Puget Sound, WA, and the study carried out at the United States Geological Survey's Marrowstone Field Station. Seawater for all aspects of the study was drawn from 150 m offshore in high current Admiralty Inlet (remote northern Puget Sound) at 17 m below mean lower low tide and treated with sand filtration and UV sterilization. Intact herring were transported on ice and dissected upon receipt for immediate fertilization. Testes were dissected from 7 males (21.6 ± 5.9 g average weight) and ovaries from 17 females (28.4 ± 6.7 g). Testes were macerated and pooled to provide sperm to fertilize all the eggs stripped and pooled from the ovaries (483 g of source tissue from the 17 females) using the poly(vinyl alcohol) method[35] to prevent clumping and control adherence while evenly distributing onto 16 21 × 24 cm sheets of 1 mm nylon mesh. Fertilized eggs were incubated overnight by suspension of mesh sheets in 4 ft diameter flow-through seawater tanks and assessed for fertilization rates before transfer to column effluent tanks. Mean fertilization success was ∼90% (n = 16 sheets, 89.4 ± 5.6%)

2.2. Oil Exposure. To produce oiled gravel effluents with relatively low dissolved PAH concentrations, we continued weathering gravel from an earlier study.[8] As described previously, gravel was coated with Alaska North Slope crude oil at three dosing levels (0.25, 0.5, and 1.0 g oil/kg gravel) and loaded into identical PVC columns (∼1000 cm^3 of gravel per column), each plumbed to flow into 114 L glass aquaria in which herring embryos were exposed. Prior to the current study, the gravel was used in 2016[8] to generate effluents at a flow rate of 3.6 L/h for a total of 26 days at 10.5 ± 0.2 °C, then stored at −20 °C for 1 year. For this study, columns were reactivated and subsequently weathered for an additional 9 days at 3.6 L/h (9.9 ± 0.2 °C) before initiating the exposure reported here.

For exposure, 4 sheets with adherent embryos were randomly selected from the pool of 16 to suspend in each of the column effluent tanks (one tank per dosing level, three oil levels plus clean gravel control). Standpipes kept the steady-state volume of the exposure tanks at ∼100 L, which were placed within larger plastic baths plumbed with high flow ambient seawater for temperature control during incubation. Column flow rates were targeted for 7.2 L/h and adjusted on a daily basis; final average flow rates were 6.7 ± 0.3 L/h for control, 7.1 ± 0.2 for 0.25, 6.9 ± 0.8 for 0.5, and 7.2 ± 0.4 for 1.0 g/kg oil. Temperature, pH, and dissolved oxygen were monitored daily and were (control) 10.0 ± 0.3 °C, 7.7 ± 0.3, and 9.3 ± 0.1 mg/L; (0.25 g/kg oil) 9.9 ± 0.2 °C, 7.7 ± 3, and 9.4 ± 0.1 mg/L; (0.5 g/kg oil) 9.9 ± 0.2 °C, 7.7 ± 0.3, and 9.3 ± 0.1 mg/L; and (1.0 g/kg oil) 9.9 ± 0.2 °C, 7.7 ± 0.3, and 9.4 ± 0.1 mg/L, respectively. At 10 dpf (exposure day 9) embryos were transferred to 760 L hatching tanks with clean seawater with flow rates of 2−4 L/min. Hatching initiated the following day (11 dpf) and was considered complete by 16 dpf. Hatching was quantified by counting empty eggshells in randomly imaged areas of each mesh sheet (n = 8 or 12).

2.3. Analytical Chemistry. 200 mL water samples (one per treatment) were collected by glass pipet from the center of aquaria on exposure days 1 and 9, stabilized with 20 mL dichloromethane and stored at 4 °C until extracted and analyzed by GC−MS as detailed elsewhere.[8,36] For body burden analyses, 100 embryos were randomly selected from the initial fertilized pool and from each exposure group at 10 dpf (exposure day 9), flash frozen on liquid nitrogen, and stored at −80 °C. Total mass of samples averaged 0.122 ± 0.052 g (s. d., N = 5). Subsequent microscale tissue extraction and GC−MS/MS analysis followed established methods.[37,38] LOQ for PAHs were based on the GC/MS response areas of calibration standards. For water analyses, calibration standards range from 0.001 to 3.00 μg/mL. With instrument injection volumes of 2 μL, the lowest quantifiable mass was 0.006 ng. With the concentration of extracts, the actual LOQ was 0.002 μg/L. If a sample analyte was not detected or had a response area less than that of the lowest concentration calibration standard, it was reported as less than the LOQ values (<LOQ). For tissue samples, LOQ values were divided by a dilution factor of 10. For ∑PAH data and PAH mixture compositional plots presented, <LOQ values were treated as zero. Method blank values were not subtracted from sample values. Complete analytical chemistry data with LOQ values are reported in Supporting Data set S1.

2.4. Biological Sampling and Measurement of Cardiac End Points. At 6 and 10 dpf, four replicate samples of 30 embryos were randomly selected from small sections cut from each of the four mesh sheets for each treatment group. Samples were flash frozen on liquid nitrogen and stored at −80 °C. Total RNA was extracted and quantitative real-time reverse-transcriptase PCR (qPCR) performed with primers for *cyp1a* and reference genes *mtm1*, *rxrba*, and *wdtc1*, with fold-change values relative to control calculated using the geometric mean of the three reference genes as detailed previously.[8] At 15 dpf, hatched larvae were randomly sampled and imaged live exactly as described previously.[8] Measurements of atrial and ventricular chamber dimensions were obtained from 40 larvae per treatment group using Fiji (previously ImageJ; https://imagej.net/).[8] Area measures for individual larvae represented the mean of three measurements taken for each video, from frames in the beginning, middle, and end sections. Precision of area measurements was 94.6% as the average standard deviation across both atrial and ventricular area measures was 5.4% of the mean values. Average standard deviations for the values from individual larvae from all treatment groups combined were 12.5 and 26.7% of the mean values for the atrium and posterior ventricle, respectively.

2.5. Data Analysis. Cardiac morphometric data were analyzed by ANOVA (α = 0.05) with Dunnett's post hoc comparison of means using JMP15 for Macintosh (SAS Institute) as were the *cyp1a* qPCR data after $\log_2$ transformation. Dose−response modeling was carried out using Prism 9 for Macintosh (GraphPad Software) and comparative methods to identify statistically robust models. Chamber dimension data from the previously published exposure[8] were reanalyzed, while previously collected *cyp1a* qPCR data was analyzed de novo along with data collected for this study.

3. RESULTS

3.1. Relationship between Measured PAH Exposures and Cytochrome P4501A Induction. In the previous study,

https://doi.org/10.1021/acs.est.3c04122
Environ. Sci. Technol. 2023, 57, 19214−19222

column effluents from weathering day 16−26 produced mean ∑PAH levels of 1.33, 1.85, and 4.51 μg/L in water (0.25, 0.5, and 1.0 g oil/kg gravel, respectively) and 64, 140, and 238 ng/g in embryo tissues,[8] all well above LOQ. In the current study, the LOQ for PAHs in water ranged from 0.0018 to 0.0037 μg/L. For ∑PAH values reported here, analytes that were below the LOQ were recorded as zero. Control water samples collected on exposure day 1 had background levels of ∑PAH at 0.079 μg/L (Figure 1A). The pattern was dominated by naphthalene and

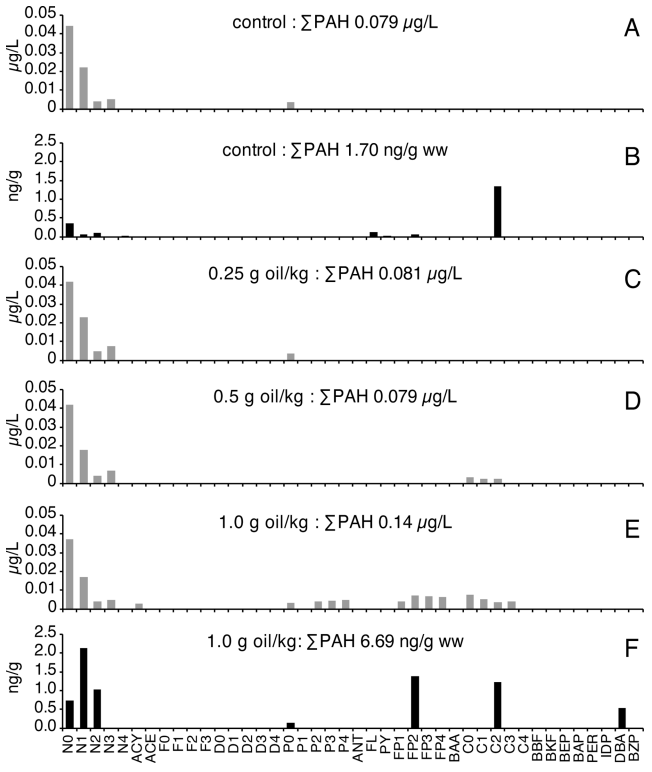

Figure 1. PAHs quantified in gravel column effluent and embryos. Concentrations of PAHs in water (μg/L) measured at exposure start are shown for (A) control, clean seawater; (C) 0.25 g/kg oil dosing level; (D) 0.5 g/kg oil dosing level; and (E) 1.0 g/kg oil dosing level. Concentrations in embryo tissues (ng/g wet weight) measured at exposure end are shown for only the control (B) and 1.0 g/kg dosing levels (F). Complete data with compounds detected < LOQ are provided in Supporting Data set S1. N, naphthalenes; ACY, acenaphthylene; ACE, acenaphthene; F, fluorene; D, dibenzothiophene; P, phenanthrene; ANT, anthracene; FL, fluoranthene; PY, pyrene; FP, fluoranthenes/pyrenes; BAA, benz[*a*]anthracene; C, chrysene; BBF, benzo[*b*]fluoranthene; BKF, benzo[*j*]fluoranthene/benzo[*k*]fluoranthene; BEP, benzo[e]pyrene; BAP, benzo[*a*]pyrene; PER, perylene; IDP, indeno[1,2,3-*cd*]pyrene; DBA, dibenz[*a*,*h*]-anthracene/dibenz[*a*,*c*]anthracene; and BZP, benzo[*ghi*]perylene. Parent compound is indicated by a 0 (e.g., N0) while numbers of additional carbons (e.g., methyl groups) for alkylated homologues are indicated as N1, N2, etc.

C1−C3 alkyl-naphthalenes with a detection of parent phenanthrene (P0). The method blank sample contained ∑PAH 0.029 μg/L, with detections of naphthalene, C3-naphthalene, and phenanthrene comparable to the control water sample (Supporting Data set S1). For the low exposure (0.25 g/kg oil dosing), the pattern of individual compounds was essentially identical to that of control water, as was measured ∑PAH (0.081 vs 0.079 μg/L; Figure 1C). The ∑PAH loading for the intermediate 0.5 g/kg oil dosing column was also indistinguishable from the control (0.079 μg/L) but included detections of parent and alkyl-chrysenes (Figure 1D). Effluent from the (relatively) high treatment (1.0 g/kg oil) column showed a ∑PAH of 0.14 μg/L with detections of alkyl-phenanthrenes/anthracenes, alkylated fluoranthene or pyrene homologues, and parent and alkylated benzanthracenes/chrysenes (Figure 1E).

For PAHs in tissues, the LOQ varied between 0.05 and 4.48 ng/g wet weight. In terms of uptake, control embryos had tissue ∑PAH levels of 1.70 ng/g at exposure day 10, with a compositional pattern of individual compounds that was similar to control exposure water with naphthalenes in addition to a trace of C2-chrysene (Figure 1B). Embryos exposed to the 0.25 and 0.5 g/kg oil dosing columns showed similarly indistinguishable tissue PAH patterns (Supporting Data set S1), with corresponding ∑PAH levels of 2.92 and 1.72 ng/g, respectively. In contrast, embryos exposed to the 1.0 g/kg oil dose had ∑PAH roughly 2 times higher than the intermediate doses at 6.69 ng/g, with a pattern dominated by alkylated naphthalenes, fluoranthene/pyrenes, and benzanthracenes/chrysenes (Figure 1F and Supporting Data set S1).

Quantitative PCR (qPCR) was used to measure the induction of *cyp1a* mRNA in response to the accumulation of PAHs in tissues during oil exposure. To more readily relate *cyp1a* induction to oil dosing, ∑PAH measurements are represented graphically for both water (Figure 2A) and embryos (Figure 2B). As expected for the normal process of weathering, measured ∑PAHs in water declined between initiation of column flow (1 dpf) and exposure end at 10 dpf. Across

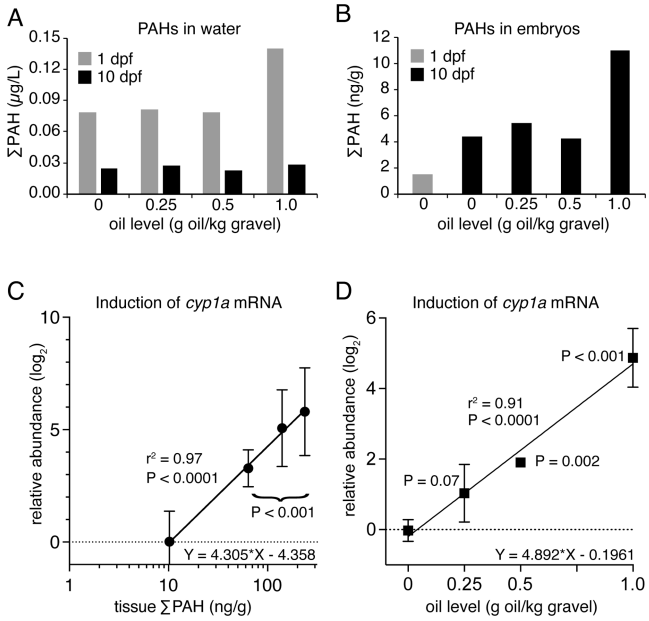

Figure 2. ∑PAH measures related to the induction of *cyp1a* mRNA. (A) ∑PAH measures (μg/L) in effluent water at start of exposure (day 1, gray bars) and at end exposure (day 10, black bars). (B) ∑PAH measures (ng/g wet weight) in embryos at start of exposure (day 1, gray bar) and at end exposure (day 10, black bars). (C,D) Relative abundance (fold-change) of *cyp1a* mRNA measured by qPCR at 10 dpf for the previously published weathering day 16−26 exposure (C) and current weathering day 35−45 exposure (D). Data points are mean ± s.e.m. ($N = 4$), and the line (with adjacent statistics) shows the simple linear regression on raw data. *P* value for ANOVA and posthoc Dunnett's test indicated for each data point.

https://doi.org/10.1021/acs.est.3c04122
Environ. Sci. Technol. 2023, 57, 19214−19222

treatments, tissue ∑PAH was generally elevated in all embryo samples relative to unexposed fertilized embryos at day 1. Following the prior exposure to the weathering day 16−26 effluents,[8] at 10 dpf there was a clear log-linear relationship (r^2 = 0.97, P < 0.0001) between levels of *cyp1a* mRNA and measured tissue ∑PAH across the dose range of 64−238 ng/g (Figure 2C). For the current exposure, we quantified *cyp1a* mRNA at the same exposure time point (10 dpf) using the same methods (Figure 2D). Although we could not measure tissue PAHs above background for the 0.25 and 0.5 g/kg exposures, there was a very similar log-linear relationship between the nominal oil loading and relative abundance of *cyp1a* mRNA (r^2 = 0.91, P < 0.0001). ANOVA and posthoc means comparisons demonstrated a clear stepwise concentration−response; the 2-fold induction of *cyp1a* mRNA in the 0.25 g/kg exposure was marginally significant (p = 0.07), while the 3.7-fold and 29-fold induction in the 0.5 g/kg (P = 0.002) and 1.0 g/kg (P < 0.001) exposures were highly significant. These two *cyp1a* stimulus−response plots thus characterize exposures that were both above and below the LOQ for PAHs, spanning the experiments in the previous (day 16−26 column effluents) and current (day 35−45 effluents) studies, respectively.

3.2. PAH Tissue Accumulation and cyp1a Induction Coincide with Heart Chamber Defects. Exposure to experimental column effluents had no impact on the viability across all four treatments. Hatch rates by 16 dpf (6 days postexposure) were 66 ± 8% in controls and 63 ± 10, 68 ± 12, and 67 ± 13% for the 0.25, 0.5, and 1.0 g/kg doses (ANOVA p = 0.7). Still frames captured from lateral-view digital videos of larvae (fifth day posthatch) were used to measure the dimensions of the atrium and posterior balloon portion of the ventricle at peak diastole (relaxed phase) for each chamber. Representative tracings of each chamber are shown for representative larvae from the control (Figure 3A) and 1.0 g/kg (Figure 3B) exposure groups. In the exposures from weathering day 16−26, there was a robust dose−response based on the measured 10 dpf embryo ∑PAH for both increase in atrial area and decrease in ventricular ballooning (ref 8 ; replotted in Figure S1). The increase in atrial area fits a linear model (r^2 = 0.70; Figure S1A), while the ventricular ballooning dose−response was nonlinear and sigmoidal (R^2 = 0.93; Figure S1B). Using *cyp1a* mRNA abundance as the exposure metric, nearly identical dose−response relationships (r^2 = 0.68 and R^2 = 0.93) were evident (Figure S1C,D). The IC_{50}s for inhibition of ventricular ballooning were ∑PAH 87 ng/g and *cyp1a* mRNA abundance of 4.3 (log_2 19.8-fold). Based on the linear equation for the *cyp1a*-∑PAH dose−response, this level of *cyp1a* induction was calculated to equal ∑PAH 103 ng/g. After the more prolonged weathering in the current exposure, the dose-dependent decrease in the lateral area of the posterior ventricle (Figure 3C, amber points) remained with a coincident increase in the area of the atrium (Figure 3C, fuchsia points). Compared to controls at 0.0068 ± 0.0012 mm^2, the posterior ventricle in the 1.0 g/kg exposure group was highly significantly reduced (by 38%; 0.0042 ± 0.0015 mm^2; p < 0.001). This disruption in ventricular morphogenesis was also significant for the 0.5 g/kg dose group (0.0061 ± 0.0017 mm^2; p = 0.04; 10% reduction) and marginal for the 0.25 g/kg dose group (0.0062 ± 0.0015 mm^2; p = 0.06). The opposite trend was evident for increase in size of the atrium (measured laterally), with controls at 0.013 ± 0.001 mm^2, and the 0.25, 0.5, and 1.0 g/kg exposures at 0.014 ± 0.002, 0.015 ± 0.002, and 0.017 ± 0.002 mm^2, respectively. Effects of the 0.5 and 1.0 g/kg exposures on the atrial area were highly significant (p = 0.002 and <0.0001, respectively). Moreover, there was a linear relationship between the area of each chamber and the relative abundance of *cyp1a* mRNA (Figure 3C, lines). The slopes were highly significant for each chamber (p < 0.0001), despite relatively low r^2 values (0.3).

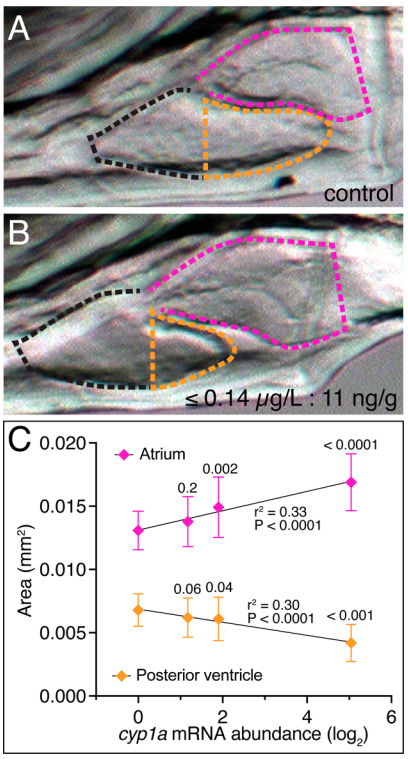

Figure 3. Relationship between cardiac chamber dimensions at hatch and *cyp1a* induction at 10 dpf. Representative lateral views of the heart in hatching stage larvae are shown for the control (A) and the 1.0 g/kg oil (∑PAH 6.69 ng/g wet weight) dosing level (B). The periphery bounding the area measures are indicated by the dashed fuchsia line for the atrium and the dashed amber line for the posterior ventricle. The unmeasured anterior extent of the ventricle is indicated by the black dashed line. Still images represent video frames taken from the diastolic phase of the ventricle. (C) Linear regression plot of atrial (fuchsia points) and posterior ventricle (amber points) lateral area measures (mm^2) against log_2 *cyp1a* mRNA relative abundance measured at 10 dpf (9 days exposure). Data represent the mean ± SD for N = 40 measures. P-values above data points represent ANOVA followed by Dunnett's post hoc test. Regression line statistics are given below and above the atrial and ventricular lines, respectively.

4. DISCUSSION

Herring and other marine forage fish are keystone species for the energy flow in coastal ecosystems worldwide. Historically, natural resource injury assessments following major oil spills have focused on the health and viability of herring early life stages in oiled nearshore spawning habitats. Despite these past efforts, the responsiveness of herring embryos to PAH mixtures at the very low end of the exposure range has not been determined. The classical oiled gravel column method was designed to produce progressively lower waterborne PAH concentrations, thereby modeling the environmental weathering of oil stranded on cobble beaches. The oiled gravel columns used here produced concentrations that ranged from a high of 4.15 μg/L[8] down to below the LOQ over a period of 45 days. On the biological response side, however, developmental cardiotoxicity remained quantifiable in corresponding embryos. Although

https://doi.org/10.1021/acs.est.3c04122
Environ. Sci. Technol. 2023, 57, 19214−19222

technical limitations precluded the direct measurement of these extremely low PAH concentrations, the direct mechanistic link between cell-internal PAH and *cyp1a* induction forms the basis for quantifying a tissue dose−response.

As shown previously in Arctic cod embryos,[32] for PAH concentrations above the LOQ, the ∑PAH-*cyp1a* dose−response effectively creates a standard curve. Subsequently, *cyp1a* mRNA levels can be used as the exposure metric for dose−response studies with toxicity end points such as impaired ventricular ballooning, as a proxy for direct quantitation of tissue PAHs. As such, there is close agreement between the above-LOQ IC_{50}s for impaired ventricular ballooning derived from measured ∑PAH (87 ng/g) and the *cyp1a* standard curve (103 ng/g). This approach is further supported at diminishing PAH concentrations by the alignment of slopes for the above-LOQ tissue ∑PAH-*cyp1a* regression line (at 4.3) and the regression line using the below-LOQ oil loadings (at 4.9). Thus, we have shown here that *cyp1a* mRNA expression provides a measurable dose−response at exposure levels for which GC−MS- and GC−MS/MS-measured water and tissue ∑PAH levels were indistinguishable from the background (water and embryos from the clean gravel treatment). At a cellular level, PAHs bind and activate the aryl hydrocarbon receptor (AHR), which in turn activates transcription of *cyp1a* mRNA.[39] In controlled oil exposure studies, the induction of *cyp1a* mRNA provides irrefutable evidence of the presence of PAHs in embryonic tissue. Its measurement here is also a testament to the exquisite sensitivity of the methods to quantifying macromolecular nucleic acids by enzymatic amplification. The stepwise induction of *cyp1a* in the below-LOQ exposures reported here are indicative of a tissue dose−response, irrespective of our inability to quantify the PAHs driving that response.

Remarkably, in terms of toxicological response, the impact on ventricular ballooning was highly significant (by ANOVA and posthoc) at the same dosing levels producing significant *cyp1a* mRNA induction. Moreover, the degree of impaired ballooning had a significant linear relationship with *cyp1a* induction. Compared to the sigmoidal dose−response observed with higher dose exposures, the linear relationship at the extreme left end of the relationship in this study likely reflects a more mild and graded disruption of ventricular morphogenesis. Both elevation of *cyp1a* mRNA and biological impacts on the developing heart provided a measurable response at exposure levels below the current limits of chemical detection. Thus, as traditionally defined by ∑PAH concentration using conventional GC/MS methods, there does not appear to be a threshold for developmental abnormalities—that is, any detectable increase in tissue PAHs above background is likely to produce critical and lasting heart defects in herring.

As a biological detector of PAHs, the AHR and its target gene *cyp1a* are more sensitive than conventional analytical chemistry in herring. Importantly, the tissue PAH data are as sensitive as is currently possible. Increasing the sensitivity of the water measures would require starting with impractically larger water samples, making extensive modifications to the current methods, or, for example, developing a new method with high-resolution mass spectrometry. Data obtained for tissue PAHs with GC−MS/MS are about 2 orders of magnitude lower than what is possible on GC−MS,[37] especially considering the low sample weights used here, around 0.1 g. The LOQs for this method correspond to subparts per billion level on the instrument. Although the quantitative methods used here differ slightly, the results from this controlled laboratory exposure are consistent with findings from field studies documenting in situ PAH exposure in caged Pacific herring embryos out-planted in the vicinity of creosote-treated pilings as part of a remediation project, to track improvements in habitat quality.[40] In that case example, herring embryos showed tissue ∑PAH levels ranging from 0.6 ng/g at a reference site to 2.7 ng/g proximal to the pilings, the latter in tandem with an approximately 2-fold increase in the relative abundance of *cyp1a* mRNA. This biomarker response was similarly elevated in herring embryos from our 0.25 and 0.5 g/kg oil treatments at day 10, which produced *cyp1a* increases of 2-fold and 4-fold, respectively, despite tissue ∑PAH levels that were indistinguishable from background controls (all at 4−5 ng/g). Thus, in both the laboratory and the field, herring *cyp1a* responds to vanishingly small traces of PAHs (and potentially other unmeasured fossil-fuel-derived CYP1A inducers) that cannot be quantified by analytical chemistry. More importantly, our current findings link modest but significant *cyp1a* induction to adverse biological impacts on heart development. This essentially indicates that any level of *cyp1a* induction in response to a known petroleum exposure during the sensitive window of cardiac organogenesis can be linked to latent reduction in individual fitness from lasting defects in heart chamber formation, validating previous suggestions.[41] Thus, in the absence of direct measures of cardiotoxicity, when used with appropriate reference samples, *cyp1a* induction alone represents a powerful tool for assessing the real-world environmental impacts of petroleum pollution in fish spawning habitats. Nevertheless, many state and Federal monitoring programs will continue to use traditional PAH analytical methods. Even with significant modifications to analytical methods, a major obstacle will continue to be the pervasiveness of abundant lower molecular weight compounds, which can be present in even ultrapure grade laboratory solvents. For laboratories in major metropolitan areas with significant airborne PAHs, these improvements are at a minimum impractical and more likely impossible. On the other hand, the sensitivity of fish embryos as integrators of exposure demonstrated here in the laboratory and in the field,[40,42] for both exposure and effect biomarkers, reinforces the advantages of biomonitoring over chemical measurements in environmental assessments of petroleum pollution impacts. Looking forward, it may be possible to develop novel, highly sensitive methods for quantifying PAHs using the PAH-inducible DNA binding/transcriptional activation function of the AHR as a biosensor.[43]

We and others have quantified a wide range of cardiotoxicity end points in oil-exposed embryos across a diversity of fish species. These metrics include edema accumulation (a measure of cardiac output), heart rate, heart rhythm, chamber contractility (measured as fractional shortening), chamber area-based volumetric cardiac output (a derivative of fractional shortening), chamber looping (atrioventricular angle), total chamber area for the atrium and ventricle, and area of the posterior ventricle (ballooning).[6,10,12,25,32,34,44,45] Among this entire suite of diagnostic indicators, the degree of ventricular ballooning at the hatch is by far the most sensitive. As shown here, perturbations to ventricular morphogenesis are on par with the sensitivity of *cyp1a* induction in herring. This finding has implications for determining which oil-sensitive intracardiac mechanisms are paramount in terms of predicting adverse outcomes at higher biological scales later in time. A precise threshold has not been established for impacts on chamber contractility (driven by Ca^{2+}-dependent myofibrillar actomyosin). However, using edema accumulation as a proxy indicator of

https://doi.org/10.1021/acs.est.3c04122
Environ. Sci. Technol. 2023, 57, 19214−19222

cardiac output failure, the threshold for contractility defects appears to be higher.[8] Embryos with a ∑PAH body burden of 1.2 μM (238 ng/g) hatched with a near-complete lack of ventricular ballooning (EC_{50} = 0.3 μM), whereas the EC_{50} for accumulation of edema was 1 μM. While ventricular ballooning is a complex process that requires the coordination of multiple Ca^{2+}-regulated mechanisms, the current findings suggest that impacts on cardiomyocyte cytoskeletal actomyosin and its attendant role in cell shape changes may be the most important driver of oil-induced defects in heart development. Importantly, abnormal expansion of the atrium is nearly as sensitive a measure of oil exposure. However, detailed analyses of atrial development in embryos and later life stages are far more challenging due to chamber structure and anatomical orientation; that is, the cellularity of the atrium is nearly impossible to assess in nonmodel species that lack transgenic fluorescent markers for use in 3-D time-lapse imaging. Nevertheless, the most parsimonious explanation for the observed atrial enlargement is dilation in response to elevated pressures arising from reduced ventricular volume.[46,47] To further explore this hypothesis, future studies of the atrium should address cellular- and molecular-level responses to petroleum-derived PAHs.

Our results do not necessarily imply that PAHs alone cause developmental toxicity from oil. As is well-known, the vast majority of compounds that remain in crude oils after weathering to remove monoaromatics are insoluble in water. For those remaining compounds that are somewhat soluble, there are two determinants for solubility: aromaticity and polarity.[48] Because methods for conventional PAH quantification were historically well-established, this purely aromatic group of compounds was readily associated with the adverse impacts of oil exposure in fish embryos in the earliest studies, which ruled out contributions from many other oil components.[17] Polar compounds could conceivably contribute to early life stage toxicity, but there have been no rigorous toxicological screens for potential candidates. Nevertheless, canonical crude oil toxicity, as characterized by dozens of studies in the years following the 1989 *Exxon Valdez* oil spill, must involve a CYP1A enzyme substrate as indicated by the *cyp1a* induction observed here together with previous evidence from *cyp1a* knockdown in zebrafish.[33] Because the CYP1A enzyme prefers planar aromatic substrates,[49,50] any compound besides PAHs that contributes to toxicity would have to be closely related in structure, for example, heterocycles or PAH-related compounds with polar functional groups. In any event, impaired ventricular ballooning in herring is (a) an extremely sensitive biological end point with a strong dose−response relationship to PAH concentrations, (b) tightly coupled to the presence of PAHs in tissues (detected either by *cyp1a* induction or GC−MS/MS), and (c) occurs at tissue concentrations that match the range of ∑PAH IC_{50}/EC_{50} measures for the rapid and direct impacts on cardiomyocyte electrophysiological and contractile functions. This effect of the crude oil is not specific to herring. Nearly identical effects were observed recently in Atlantic haddock following embryonic exposure to a geologically distinct crude oil.[13] The thresholds for these two species are likely to be similar as a lower no-effect threshold was not reached at a tissue level of 27 ng/g of ∑PAH in the haddock study. These findings reinforce the central role of PAHs as major determinants of the developmental toxicity of crude oil to fish.

Finally, our results have important implications for both risk and damage assessments in aquatic habitats at risk from petroleum pollution from a variety of environmental sources beyond oil spills. For example, identical effects on heart development were observed in Pacific herring embryos exposed to highway runoff containing PAHs at similar levels to oiled gravel effluents.[51] The < LOQ ∑PAH threshold for impairment of heart development in herring suggests that even the low levels of PAHs associated with urbanized nearshore areas impacted by nonpoint PAH sources could be limiting local population productivity.[52] In the context of the original controversy surrounding the immediate impacts of the *Exxon Valdez* spill on herring in Prince William Sound and the subsequent collapse of the population,[53] the toxicity of petroleum to developing fish continues to be underestimated.

■ ASSOCIATED CONTENT

Supporting Information

The Supporting Information is available free of charge at https://pubs.acs.org/doi/10.1021/acs.est.3c04122.

Complete results of PAH analyses in water and embryos (XLSX)

Dose−response relationships for cardiac chamber dimensions and above-LOQ tissue ∑PAH concentrations and cyp1a mRNA levels (PDF)

■ AUTHOR INFORMATION

Corresponding Author

John P. Incardona − *National Oceanic and Atmospheric Administration, Northwest Fisheries Science Center, Seattle, Washington 98112, United States;* orcid.org/0000-0002-1093-3408; Email: john.incardona@noaa.gov

Authors

Tiffany L. Linbo − *National Oceanic and Atmospheric Administration, Northwest Fisheries Science Center, Seattle, Washington 98112, United States*

James R. Cameron − *National Oceanic and Atmospheric Administration, Saltwater, Inc., under Contract to Northwest Fisheries Science Center, Seattle, Washington 98112, United States*

Barbara L. French − *National Oceanic and Atmospheric Administration, Northwest Fisheries Science Center, Seattle, Washington 98112, United States;* orcid.org/0000-0002-2358-9044

Jennie L. Bolton − *National Oceanic and Atmospheric Administration, Northwest Fisheries Science Center, Seattle, Washington 98112, United States*

Jacob L. Gregg − *Marrowstone Marine Field Station, US Geological Survey, Western Fisheries Research Center, Nordland, Washington 98358-9633, United States*

Carey E. Donald − *Institute of Marine Research, Bergen, Nordnes 5817, Norway;* orcid.org/0000-0002-1246-2961

Paul K. Hershberger − *Marrowstone Marine Field Station, US Geological Survey, Western Fisheries Research Center, Nordland, Washington 98358-9633, United States*

Nathaniel L. Scholz − *National Oceanic and Atmospheric Administration, Northwest Fisheries Science Center, Seattle, Washington 98112, United States;* orcid.org/0000-0001-6207-0272

Complete contact information is available at: https://pubs.acs.org/10.1021/acs.est.3c04122

Author Contributions

The manuscript was written through contributions of all authors. All authors have given approval to the final version of the manuscript. J.P.I. obtained funding, managed the project, designed and executed the study, analyzed data, and drafted the manuscript; T.L.L. coordinated study execution, executed the study, and analyzed the data; J.C. executed the study and analyzed the data; B.L.F. executed the study and analyzed the data; J.L.B. analyzed data, assured data quality, and edited the manuscript; J.L.G. designed and executed the study; C.D. executed the study and analyzed the data; P.K.H. obtained funding, managed the project, and designed the study; N.L.S obtained funding, managed the project, and edited the manuscript.

Funding

This research was funded in part by the NOAA National Ocean Service Office of Response and Restoration, the Prince William Sound Regional Citizens Advisory Council, the Exxon Valdez Oil Spill Trustee Council, and the Research Council of Norway (Project #267820, EGGTOX).

Notes

The authors declare no competing financial interest.

■ ACKNOWLEDGMENTS

We thank Jim West for providing ripe herring; Cathy Laetz, Julann Spromberg, Jana Labenia, Sarah Harrison, Karen Peck, and Daryle Boyd for assistance with study execution; and Denis DaSilva for critical comments on the manuscript.

■ ABBREVIATIONS

CYP1A, cytochrome P4501A; dpf, days post fertilization; GC−MS, gas chromatography−mass spectrometry; PAH, polycyclic aromatic hydrocarbons; WAF, water-accommodated fraction

■ REFERENCES

(1) Carls, M. G.; Marty, G. D.; Hose, J. E. Synthesis of the toxicological impacts of the Exxon Valdez oil spill on Pacific herring (Clupea pallasi) in Prince William Sound, Alaska, U.S.A. *Can. J. Fish. Aquat. Sci.* **2002**, *59*, 153−172.

(2) Carls, M. G.; Rice, S. D.; Hose, J. E. Sensitivity of fish embryos to weathered crude oil: Part I. Low-level exposure during incubation causes malformations, genetic damage, and mortality in larval Pacific herring (Clupea pallasi). *Environ. Toxicol. Chem.* **1999**, *18*, 481−493.

(3) Marty, G. D.; Hose, J. E.; McGurk, M. D.; Brown, E. D.; Hinton, D. E. Histopathology and cytogenetic evaluation of Pacific herring larvae exposed to petroleum hydrocarbons in the laboratory or in Prince William Sound, Alaska, after the Exxon Valdez oil spill. *Can. J. Fish. Aquat. Sci.* **1997**, *54*, 1846−1857.

(4) Pearson, W. H.; Elston, R. A.; Bienert, R. W.; Drum, A. S.; Antrim, L. D. Why did the Prince William Sound, Alaska, Pacific herring (Clupea pallasi) fisheries collapse in 1993 and 1994? Review of hypotheses. *Can. J. Fish. Aquat. Sci.* **1999**, *56*, 711−737.

(5) Pearson, W. H.; Moksness, E.; Skalski, J. R. A Field and Laboratory Assessment of Oil-Spill Effects on Survival and Reproduction of Pacific Herring Following the Exxon Valdez Spill. *Exxon Valdez Oil Spill: Fate and Effects in Alaskan Waters*; ASTM International, 1995.

(6) Incardona, J. P.; Carls, M. G.; Day, H. L.; Sloan, C. A.; Bolton, J. L.; Collier, T. K.; Scholz, N. L. Cardiac arrhythmia is the primary response of embryonic Pacific herring (Clupea pallasi) exposed to crude oil during weathering. *Environ. Sci. Technol.* **2009**, *43*, 201−207.

(7) Incardona, J. P.; Carls, M. G.; Holland, L.; Linbo, T. L.; Baldwin, D. H.; Myers, M. S.; Peck, K. A.; Tagal, M.; Rice, S. D.; Scholz, N. L. Very low embryonic crude oil exposures cause lasting cardiac defects in salmon and herring. *Sci. Rep.* **2015**, *5*, 13499.

(8) Incardona, J. P.; Linbo, T. L.; French, B. L.; Cameron, J.; Peck, K. A.; Laetz, C. A.; Hicks, M.; Hutchinson, G.; Allan, S. E.; Boyd, D. T.; Ylitalo, G. M.; Scholz, N. L. Low-level embryonic crude oil exposure disrupts ventricular ballooning and subsequent trabeculation in Pacific herring. *Aquat. Toxicol.* **2021**, *235*, 105810.

(9) Edmunds, R. C.; Gill, J. A.; Baldwin, D. H.; Linbo, T. L.; French, B. L.; Brown, T. L.; Esbaugh, A. J.; Mager, E. M.; Stieglitz, J. D.; Hoenig, R.; Benetti, D. D.; Grosell, M.; Scholz, N. L.; Incardona, J. P. Corresponding morphological and molecular indicators of crude oil toxicity to the developing hearts of mahi mahi. *Sci. Rep.* **2015**, *5*, 17326.

(10) Incardona, J. P.; Gardner, L. D.; Linbo, T. L.; Brown, T. L.; Esbaugh, A. J.; Mager, E. M.; Stieglitz, J. D.; French, B. L.; Labenia, J. S.; Laetz, C. A.; Tagal, M.; Sloan, C. A.; Elizur, A.; Benetti, D. D.; Grosell, M.; Block, B. A.; Scholz, N. L. Deepwater Horizon Crude Oil Impacts the Developing Hearts of Large Predatory Pelagic Fish. *Proc. Natl. Acad. Sci. U.S.A.* **2014**, *111*, No. E1510.

(11) Jung, J. H.; Kim, M.; Yim, U. H.; Ha, S. Y.; Shim, W. J.; Chae, Y. S.; Kim, H.; Incardona, J. P.; Linbo, T. L.; Kwon, J. H. Differential Toxicokinetics Determines the Sensitivity of Two Marine Embryonic Fish Exposed to Iranian Heavy Crude Oil. *Environ. Sci. Technol.* **2015**, *49*, 13639−13648.

(12) Morris, J.; Gielazyn, M.; Krasnec, M.; Takeshita, R.; Forth, H.; Labenia, J. S.; Linbo, T. L.; French, B. L.; Gill, J. A.; Baldwin, D. H.; Scholz, N. L.; Incardona, J. P. Crude oil cardiotoxicity to red drum embryos is independent of oil dispersion energy. *Chemosphere* **2018**, *213*, 205−214.

(13) Sørhus, E.; Sørensen, L.; Grøsvik, B. E.; Le Goff, J.; Incardona, J. P.; Linbo, T. L.; Baldwin, D. H.; Karlsen, O.; Nordtug, T.; Hansen, B. H.; Thorsen, A.; Donald, C. E.; van der Meeren, T.; Robson, W.; Rowland, S. J.; Rasinger, J. D.; Vikebø, F. B.; Meier, S. Crude oil exposure of early life stages of Atlantic haddock suggests threshold levels for developmental toxicity as low as 0.1 μg total polyaromatic hydrocarbon (TPAH)/L. *Mar. Pollut. Bull.* **2023**, *190*, 114843.

(14) Incardona, J. P. Molecular mechanisms of crude oil developmental toxicity in fish. *Arch. Environ. Contam. Toxicol.* **2017**, *73*, 19−32.

(15) Incardona, J. P.; Scholz, N. L. The influence of heart developmental anatomy on cardiotoxicity-based adverse outcome pathways in fish. *Aquat. Toxicol.* **2016**, *177*, 515−525.

(16) Incardona, J. P.; Scholz, N. L. Case study: the 2010 Deepwater Horizon oil spill. In *Development, Physiology, and Environment: A Synthesis*; Burggren, W., Dubansky, B., Eds.; Springer: London, 2018.

(17) Marty, G. D.; Hinton, D. E.; Short, J. W.; Heintz, R. A.; Rice, S. D.; Dambach, D. M.; Willits, N. H.; Stegeman, J. J. Ascites, premature emergence, increased gonadal cell apoptosis, and cytochrome P4501A induction in pink salmon larvae continuously exposed to oil-contaminated gravel during development. *Can. J. Zool.* **1997**, *75*, 989−1007.

(18) Short, J. W.; Harris, P. M. Chemical sampling and analysis of petroleum hydrocarbons in near-surface seawater of Prince William Sound after the Exxon Valdez oil spill. In *Am. Fish S S*; Rice, S. D., Spies, R. B., Wolfe, D. A., Wright, B. A., Eds., 1996; Vol. *18*, pp 17−28.

(19) Short, J. W.; Heintz, R. A. Identification of Exxon Valdez oil in sediments and tissues from Prince William Sound and the Northwestern Gulf of Alaska based on a PAH weathering model. *Environ. Sci. Technol.* **1997**, *31*, 2375−2384.

(20) Morales-Caselles, C.; Jiménez-Tenorio, N.; de Canales, M. L. G.; Sarasquete, C.; DelValls, T. A. Ecotoxicity of Sediments Contaminated by the Oil Spill Associated with the Tanker "Prestige" Using Juveniles of the Fish Sparus aurata. *Arch. Environ. Contam. Toxicol.* **2006**, *51*, 652−660.

(21) Donohoe, R. M.; Duke, B. M.; Clark, S. L.; Joab, B. M.; Dugan, J. E.; Hubbard, D. M.; DaSilva, A. R.; Anderson, M. J. Toxicity of Refugio Beach Oil to Sand Crabs (Emerita analoga), Blue Mussels (Mytilus sp.), and Inland Silversides (Menidia beryllina). *Environ. Toxicol. Chem.* **2021**, *40*, 2578−2586.

(22) Singleman, C.; Holtzman, N. G. Analysis of postembryonic heart development and maturation in the zebrafish, Danio rerio. *Dev. Dynam.* **2012**, *241*, 1993−2004.

(23) Brette, F.; Machado, B.; Cros, C.; Incardona, J. P.; Scholz, N. L.; Block, B. A. Crude oil impairs cardiac excitation-contraction coupling in fish. *Science* **2014**, *343*, 772−776.
(24) Cypher, A. D.; Linbo, T. L.; Cameron, J.; Gill, J. A.; Peck, K. A.; Gregg, J. L.; Hershberger, P. K.; Whitehead, A.; Scholz, N. L.; Incardona, J. P. Crude oil-induced cardiotoxicity during embryonic development varies with source population at hatch in Pacific herring. **2023**, In prep.
(25) Sørhus, E.; Incardona, J. P.; Karlsen, Ø.; Linbo, T. L.; Sørensen, L.; Nordtug, T.; van der Meeren, T.; Thorsen, A.; Thorbjørnsen, M.; Jentoft, S.; Edvardsen, R. B.; Meier, S. Crude oil exposures reveal roles for intracellular calcium cycling in haddock craniofacial and cardiac development. *Sci. Rep.* **2016**, *6*, 31058.
(26) Sidhwani, P.; Yelon, D. Chapter Eleven - Fluid forces shape the embryonic heart: Insights from zebrafish. In *Current Topics in Developmental Biology*; Wellik, D. M., Ed.; Academic Press, 2019; Vol. *132*, pp 395−416.
(27) Staudt, D.; Stainier, D. Uncovering the molecular and cellular mechanisms of heart development using the zebrafish. *Annu. Rev. Genet.* **2012**, *46*, 397−418.
(28) Collins, M. M.; Stainier, D. Y. Organ Function as a Modulator of Organ Formation: Lessons from Zebrafish. *Curr. Top. Dev. Biol.* **2016**, *117*, 417−433.
(29) Abdul-Wajid, S.; Demarest, B. L.; Yost, H. J. Loss of embryonic neural crest derived cardiomyocytes causes adult onset hypertrophic cardiomyopathy in zebrafish. *Nat. Commun.* **2018**, *9*, 4603.
(30) Sehnert, A. J.; Huq, A.; Weinstein, B. M.; Walker, C.; Fishman, M.; Stainier, D. Y. Cardiac troponin T is essential in sarcomere assembly and cardiac contractility. *Nat. Genet.* **2002**, *31*, 106−110.
(31) Esbaugh, A. J.; Mager, E. M.; Stieglitz, J. D.; Hoenig, R.; Brown, T. L.; French, B. L.; Linbo, T. L.; Lay, C.; Forth, H.; Scholz, N. L.; Incardona, J. P.; Morris, J. M.; Benetti, D. D.; Grosell, M. The effects of weathering and chemical dispersion on Deepwater Horizon crude oil toxicity to mahi-mahi (Coryphaena hippurus) early life stages. *Sci. Total Environ.* **2016**, *543*, 644−651.
(32) Laurel, B. J.; Copeman, L.; Iseri, P.; Spencer, M.; Hutchinson, G.; Nordtug, T.; Donald, C.; Meier, S.; Allan, S. E.; Boyd, D.; Ylitalo, G.; Cameron, J.; French, B.; Linbo, T.; Scholz, N. L.; Incardona, J. P. Embryonic crude oil exposure impairs growth and lipid allocation in a keystone Arctic forage fish. *iScience* **2019**, *19*, 1101−1113.
(33) Hicken, C. E.; Linbo, T. L.; Baldwin, D. H.; Willis, M. L.; Myers, M. S.; Holland, L.; Larsen, M.; Stekoll, M. S.; Rice, S. D.; Collier, T. K.; Scholz, N. L.; Incardona, J. P. Sub-lethal exposure to crude oil during embryonic development alters cardiac morphology and reduces aerobic capacity in adult fish. *Proc. Natl. Acad. Sci. U.S.A.* **2011**, *108*, 7086−7090.
(34) Incardona, J. P.; Carls, M. G.; Teraoka, H.; Sloan, C. A.; Collier, T. K.; Scholz, N. L. Aryl hydrocarbon receptor-independent toxicity of weathered crude oil during fish development. *Environ. Health Perspect.* **2005**, *113*, 1755−1762.
(35) Griffin, F. J.; Pillai, M. C.; Vines, C. A.; Kaaria, J.; Hibbard-Robbins, T.; Yanagimachi, R.; Cherr, G. N. Effects of salinity on sperm motility, fertilization, and development in the Pacific herring, Clupea pallasi. *Biol. Bull.* **1998**, *194*, 25−35.
(36) Sloan, C. A.; Anulacion, B. F.; Baugh, K. A.; Bolton, J. L.; Boyd, D.; Boyer, R. H.; Burrows, D. G.; Herman, D. P.; Pearce, R. W.; Ylitalo, G. M.. *Northwest Fisheries Science Center's Analyses of Tissue, Sediment, and Water Samples for Organic Contaminants by Gas Chromatography/Mass Spectrometry and Analyses of Tissue for Lipid Classes by Thin Layer Chromatogrphy/Flame Ionization Detection*, 2014; p 61.
(37) Sørensen, L.; Meier, S.; Mjøs, S. A. Application of gas chromatography/tandem mass spectrometry to determine a wide range of petrogenic alkylated polycyclic aromatic hydrocarbons in biotic samples. *Rapid Commun. Mass Spectrom.* **2016**, *30*, 2052−2058.
(38) Sørensen, L.; Silva, M. S.; Booth, A. M.; Meier, S. Optimization and comparison of miniaturized extraction techniques for PAHs from crude oil exposed Atlantic cod and haddock eggs. *Anal. Bioanal. Chem.* **2016**, *408*, 1023−1032.
(39) Barouki, R.; Aggerbeck, M.; Aggerbeck, L.; Coumoul, X. The aryl hydrocarbon receptor system. *Drug Metab. Pers. Ther.* **2012**, *27*, 3−8.
(40) West, J. E.; Carey, A. J.; Ylitalo, G. M.; Incardona, J. P.; Edmunds, R. C.; Sloan, C. A.; Niewolny, L. A.; Lanksbury, J. A.; O'Neill, S. M. Polycyclic aromatic hydrocarbons in Pacific herring (Clupea pallasii) embryos exposed to creosote-treated pilings during a piling-removal project in a nearshore marine habitat of Puget Sound. *Mar. Pollut. Bull.* **2019**, *142*, 253−262.
(41) Carls, M. G.; Heintz, R. A.; Marty, G. D.; Rice, S. D. Cytochrome P4501A induction in oil-exposed pink salmon Oncorhynchus gorbuscha embryos predicts reduced survival potential. *Mar. Ecol.: Prog. Ser.* **2005**, *301*, 253−265.
(42) Incardona, J. P.; Vines, C. A.; Anulacion, B. F.; Baldwin, D. H.; Day, H. L.; French, B. L.; Labenia, J. S.; Linbo, T. L.; Myers, M. S.; Olson, O. P.; Sloan, C. A.; Sol, S.; Griffin, F. J.; Menard, K.; Morgan, S. G.; West, J. E.; Collier, T. K.; Ylitalo, G. M.; Cherr, G. N.; Scholz, N. L. Unexpectedly high mortality in Pacific herring embryos exposed to the 2007 Cosco Busan oil spill in San Francisco Bay. *Proc. Natl. Acad. Sci. U.S.A.* **2012**, *109*, E51−E58.
(43) Tellechea-Luzardo, J.; Stiebritz, M. T.; Carbonell, P. Transcription factor-based biosensors for screening and dynamic regulation. *Front. Bioeng. Biotechnol.* **2023**, *11*, 1118702.
(44) Jung, J.-H.; Hicken, C. E.; Boyd, D.; Anulacion, B. F.; Carls, M. G.; Shim, W. J.; Incardona, J. P. Geologically distinct crude oils cause a common cardiotoxicity syndrome in developing zebrafish. *Chemosphere* **2013**, *91*, 1146−1155.
(45) Khursigara, A. J.; Perrichon, P.; Martinez Bautista, N.; Burggren, W. W.; Esbaugh, A. J. Cardiac function and survival are affected by crude oil in larval red drum, Sciaenops ocellatus. *Sci. Total Environ.* **2017**, *579*, 797−804.
(46) Kamel, S. M.; Koopman, C. D.; Kruse, F.; Willekers, S.; Chocron, S.; Bakkers, J. A Heterozygous Mutation in Cardiac Troponin T Promotes Ca^{2+} Dysregulation and Adult Cardiomyopathy in Zebrafish. *J. Cardiovasc. Dev. Dis.* **2021**, *8*, 46.
(47) Thomas, L.; Abhayaratna, W. P. Left Atrial Reverse Remodeling: Mechanisms, Evaluation, and Clinical Significance. *JACC: Cardiovasc. Imag.* **2017**, *10*, 65−77.
(48) Liu, Y.; Kujawinski, E. B. Chemical Composition and Potential Environmental Impacts of Water-Soluble Polar Crude Oil Components Inferred from ESI FT-ICR MS. *PLoS One* **2015**, *10*, No. e0136376.
(49) Lewis, D. F. V.; Eddershaw, P. J.; Dickins, M.; Tarbit, M. H.; Goldfarb, P. S. Structural determinants of cytochrome P450 substrate specificity, binding affinity and catalytic rate. *Chem. Biol. Interact.* **1998**, *115*, 175−199.
(50) Urban, P.; Truan, G.; Pompon, D. Differences in functional clustering of endogenous and exogenous substrates between members of the CYP1A subfamily. *Open Drug Metabol. J.* **2009**, *3*, 17−30.
(51) Harding, L. B.; Tagal, M.; Ylitalo, G. M.; Incardona, J. P.; Davis, J. W.; Scholz, N. L.; McIntyre, J. K. Urban stormwater and crude oil injury pathways converge on the developing heart of a shore-spawning marine forage fish. *Aquat. Toxicol.* **2020**, *229*, 105654.
(52) West, J. E.; O'Neill, S. M.; Ylitalo, G. M.; Incardona, J. P.; Doty, D. C.; Dutch, M. E. An evaluation of background levels and sources of polycyclic aromatic hydrocarbons in naturally spawned embryos of Pacific herring (Clupea pallasii) from Puget Sound, Washington, USA. *Sci. Total Environ.* **2014**, *499*, 114−124.
(53) Boehm, P. D.; Neff, J. M.; Page, D. S. Assessment of polycyclic aromatic hydrocarbon exposure in the waters of Prince William Sound after the Exxon Valdez oil spill: 1989−2005. *Mar. Pollut. Bull.* **2007**, *54*, 339−356.

https://doi.org/10.1021/acs.est.3c04122
Environ. Sci. Technol. 2023, 57, 19214−19222